

Surface structure of single-crystal cubic boron nitride (111) studied by LEED, EELS, and AES

Kian Ping Loh, Isao Sakaguchi, and Mikka Nishitani-Gamo

Core Research for Evolutional Science and Technology (CREST), Japan Science and Technology Corporation (JST),
c/o National Institute for Research in Inorganic Materials (NIRIM), 1-1 Namiki, Tsukuba, Ibaraki 305, Japan

Takashi Taniguchi

National Institute for Research in Inorganic Materials (NIRIM), 1-1 Namiki, Tsukuba, Ibaraki 305, Japan

Toshihiro Ando*

Core Research for Evolutional Science and Technology (CREST), Japan Science and Technology Corporation (JST)
and National Institute for Research in Inorganic Materials (NIRIM), 1-1 Namiki, Tsukuba, Ibaraki 305, Japan

(Received 11 July 1997; revised manuscript received 4 September 1997)

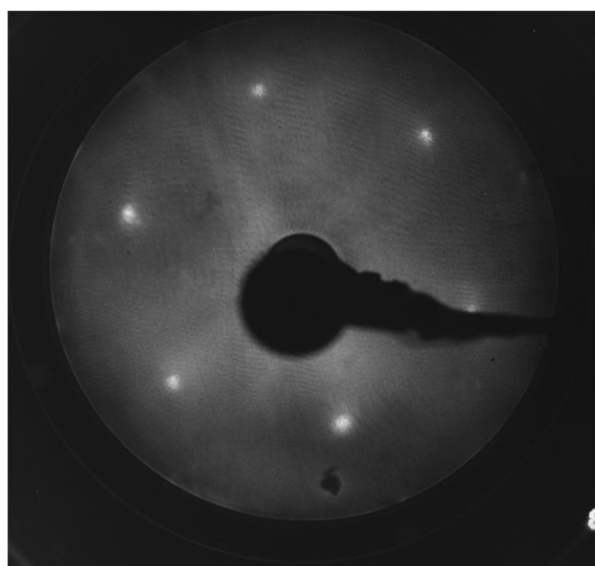
The surface symmetry of cubic boron nitride (111) (*c*-BN) is characterized by low-electron energy diffraction. The polished *c*-BN (111) and hydrogen-plasma-treated sample both exhibit a 1×1 surface structure. The surface is effectively etched by hydrogen plasma. High-resolution Auger and electron-energy-loss spectroscopy studies confirmed that the hydrogen-etched surface retains the integrity of crystalline *c*-BN (111). Characteristic energy-loss peaks at 15 eV due to an interband transition and at 37 eV due to a bulk plasmon can be observed on the single-crystal surface, even though they are usually absent from the energy-loss spectra of pyrolytic or polycrystalline BN samples. [S0163-1829(97)52444-1]

Cubic BN (*c*-BN) is the analog of diamond and is the second hardest material following diamond. Potentially, *c*-BN thin films can have wide-ranging applications that include wide band-gap semiconductors,^{1,2} heat sinks, cutting tools, and field-emission devices.³ In practice, however, the synthesis of high-quality *c*-BN thin film is more difficult even than that of diamond. To date, vapor phase deposition methods generally give rise to nanocrystalline material with mixed sp^2 and sp^3 content in contrast to the well-developed habits now routinely observed in diamond chemical vapor deposition (CVD). One reason is that in the case of *c*-BN growth, it is not clear whether a route exists whereby the sp^3 phase can be promoted selectively by some precursors, in analogy to the role played by atomic hydrogen in maintaining the sp^3 integrity on the diamond surface during CVD growth.⁴ Currently, there is a lack of information about the surface structure of *c*-BN as well as its reactivity with simple molecules. Information regarding the reactive chemistry of *c*-BN with potential sp^2 etchants⁵ such as atomic hydrogen is vital for the development of new growth techniques employing gas phase chemical beams, as well as for the future processing of semiconductor devices based on *c*-BN. The largest difficulty facing *c*-BN research is the lack of high-quality semiconducting crystals of a sufficient size (>0.3 mm) that can be readily studied by conventional surface science techniques. Recently, one of us succeeded in growing high-quality Be-doped *c*-BN on diamond under high-pressure and high-temperature conditions by exploiting the excellent lattice match between diamond and *c*-BN.^{6,7} In this paper, we present data on the surface symmetry and morphology of the hydrogen-treated *c*-BN (111) surface.

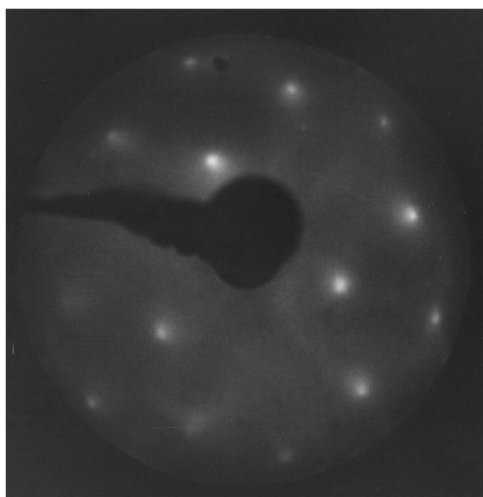
Be-doped single-crystal *c*-BN (1 mm \times 1 mm) was heteroepitaxially grown on the (111) face of diamond seed crystal by the temperature gradient method in a modified belt-type high-pressure apparatus as reported previously.⁷ The

color of the crystal was deep blue. The as-grown sample appeared to be macroscopically rough and was polished with diamond abrasives to obtain an optical finish and degreased in an ethanol ultrasonicator before its introduction into a UHV chamber equipped with low-electron energy diffraction (LEED) and Auger electron spectroscopy (AES). The UHV chamber is coupled to a microwave CVD system, where the samples can be introduced into a vacuum for treatment with pure hydrogen plasma using a microwave power of 800 W, a H_2 flow rate of 400 sccm, a gas pressure of 40 Torr, and at an average temperature of 750 °C for 10–30 min. High-resolution Auger spectra were collected using a concentric hemispherical analyzer and with an electron-beam energy of 2 KeV, a beam current of 2 nA on a spot size of 100 μ m. Electron-energy-loss spectroscopy (EELS) was performed with an electron-beam energy of 1000 eV. Commercially available highly oriented pyrolytic hexagonal BN (Denka Co.) was used as the sample for comparative spectroscopic studies.

After the polished *c*-BN (111) sample was installed in the UHV, a weak, diffuse, sixfold symmetry LEED pattern could be obtained directly. AES analysis reveals that approximately 20% of the surface was contaminated with carbon. Heating the sample to the highest achievable temperature of 900 °C in our system did not result in any change in the observed LEED pattern, indicating that the species that terminate the surface and maintain the 1×1 symmetry remain stable at 900 °C. After hydrogen-plasma treatment, the 1×1 pattern remains but the sharpness of the LEED spots was observed to improve significantly, as shown in Figs. 1(a) and 1(b). All traces of surface carbon were removed after the hydrogen-plasma treatment was verified by AES. The surface unit mesh obtained from the observed LEED pattern was found to agree with that of the bulk cubic (111) spacing, as opposed to the alternative pattern consisting of recon-



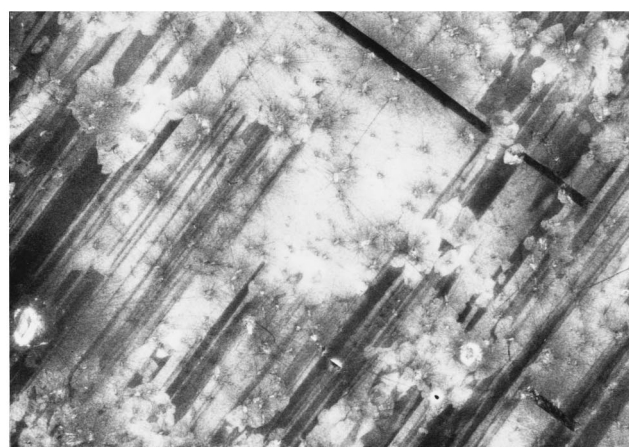
(a)



(b)

FIG. 1. LEED pattern showing sixfold symmetry spots after hydrogen-plasma treatment using primary beam energy of (a) 150 eV and (b) 325 eV.

structured 2×1 or 2×2 structure.⁸ A scanning electron micrograph of the sample before and after hydrogen-plasma treatment is shown in Figs. 2(a) and 2(b) to reveal the breaking up of the larger terraces into highly oriented smaller triangular pyramids or terraces. The surface also appears to be “macroscopically” rougher, which is evident of the etching effect of atomic hydrogen on *c*-BN. Obviously, reduction in the terrace size did not destroy the diffraction pattern characteristic of the regular 1×1 structure. In fact, LEED spots could now be observed at primary energy (E_p) as low as 70 eV, suggesting that the small triangular terraced structures produced by hydrogen etching are the same as the regular domain structure and smoother on an atomic scale. Another possibility we must consider carefully is that the observed 1×1 hexagonal surface mesh is due to hexagonal BN (*h*-BN), produced after hydrogen-plasma and high-temperature induced transformation of the surface *c*-BN layers. A monolayer of quasiepitaxially oriented *h*-BN will re-



(a)

30.0 μm



(b)

30.0 μm

FIG. 2. SEM pictures showing *c*-BN surface (a) before and (b) after hydrogen-plasma etching.

sult in slight radial streaking of the integral order due to the close lattice match. However, if the *h*-BN layer is oriented randomly or at an angle with respect to the substrate bulk, rings or a superimposed 1×1 pattern will result. In the present case, LEED features originating from a *h*-BN overlayer on the *c*-BN crystal, such as radial streaking of the spots, formation of rings, or superimposed 1×1 spots, were not observed. Therefore, if the spots were due to *h*-BN, there remained only the possibility that the *h*-BN overlayer was more than a few layers thick, in which case its presence could be easily detected by AES and EELS. For example, the mean free path for the B core-valence-valence (KVV) Auger electron is about 6 Å (kinetic energy ~ 170 eV) (Ref. 9) and its line shape will be characteristic of the bonding up to a depth of 2–3 interatomic distances from the surface.

Previous studies by Lurie and Wilson on diamond/graphite¹⁰ and Trhan and co-workers on pyrolytic *c*-BN/*h*-BN (Ref. 11) have shown that the Auger transitions of the core-valence-valence type (KVV) can provide a fingerprint for the various allotropes and can be interpreted based on the self-convolution of the valence-band density of states (DOS) of the solids. Information about the surface

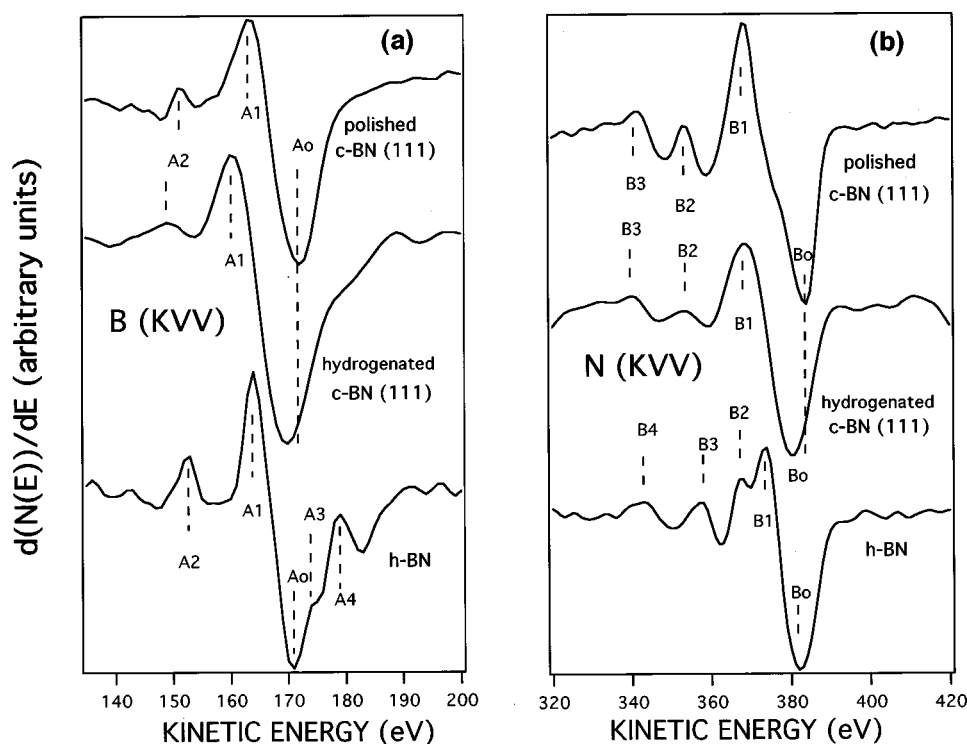


FIG. 3. High-resolution (a) B-KVV and (b) N-KVV Auger spectra of polished *c*-BN, hydrogenated *c*-BN, and hexagonal BN.

bonding state, the chemical environment, and the orbital symmetry about the core-hole site is well manifested in the KVV Auger line shape. Figures 3(a) and 3(b) show the B $1s$ and N $1s$ KVV Auger transitions of the polished sample, the hydrogen-plasma-treated sample and highly ordered pyrolytic *h*-BN. It is clear that several features distinguish the polished and hydrogen-plasma-treated *c*-BN surface from *h*-BN. Firstly, the peak width of the various peaks in *c*-BN spectra of both polished and hydrogen-plasma-treated surfaces are broader and less well-resolved compared to the narrower peaks in *h*-BN. This reflects the sharper valence-band edges and sharper DOS band structures of *h*-BN compared to *c*-BN.¹² The most distinguishing feature is the presence of peaks A_3 and A_4 [Fig. 3(a)] assignable to interatomic Auger transition $K^B L_{2,3}^N L_{2,3}^N$ in the B-KVV of *h*-BN (Ref. 11) and peak B_2 [Fig. 3(a)] in the N-KVV spectra of *h*-BN, all of which are conspicuously absent from the *c*-BN spectra. Peak B_2 , a characteristic feature in the N-KVV spectrum of *h*-BN, can be assigned to the π plasmon loss suffered by the main peak B_0 , as its position is about 9 eV lower. Based on the fact that the hydrogenated *c*-BN shows sharp LEED spots, we would recommend the presence of a broad A_2 peak as well as weak A_2 -to- A_1 peak ratio in the B-KVV spectrum (corresponding peak B_2 in N-KVV) as a quality factor for *c*-BN, as further comparison with reported argon-ion irradiated amorphous BN KVV spectra show that a strong and sharp A_2 (or B_2) peak is characteristic of a higher sp^2 content or a disordered phase.¹¹ The AES main peak position (A_0) of the polished *c*-BN has shifted by 1.2 eV towards lower kinetic energy after hydrogen-plasma treatment, probably due to a shift in the valence-band DOS maximum towards lower energies with respect to the core level after complete hydrogen termination of the surface. Similar shifts reflecting hydrogen-coverage-dependent movement of Auger

peaks have been reported by Krainisky and co-workers¹³ for diamond with varying hydrogen coverage.

EELS spectra of the hydrogen-plasma-treated *c*-BN and *h*-BN are shown in Figs. 4(a) and 4(b), respectively, for comparison. It is clear that the positions of the energy-loss peaks of the *c*-BN sample differ remarkably from *h*-BN. The peak at 8 eV for the *h*-BN EELS spectrum in Fig. 4(b) assignable to the $\pi \rightarrow \pi^*$ transition is conspicuously absent from the *c*-BN EELS spectrum [Fig. 4(a)], thus confirming the absence of sp^2 -type bonding on the hydrogen-plasma-treated *c*-BN surface. Based on the reflectivity data of Phillip and Taft,¹⁴ which reported a prominent peak at 14.5 eV, we

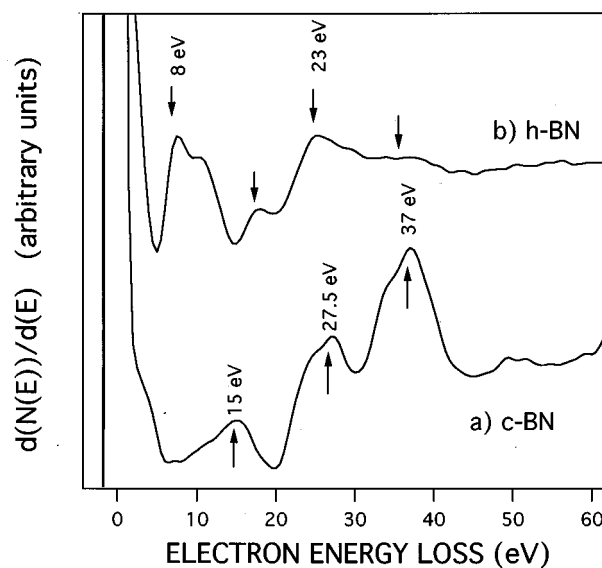


FIG. 4. EELS spectrum of (a) *c*-BN and (b) *h*-BN presented in the $d[N(E)]/d(E)$ mode.

assigned the 15 eV peak to an interband transition between the valence band and high-energy conduction band. The peaks at 27.5 and 37 eV in Fig. 4(a) are plasmon peaks in agreement with theoretical energy-loss calculations.¹² The strong 37 eV plasmon peak in particular is a fingerprint of a good sp^3 crystalline phase as it is usually not observed on pyrolytic c -BN (Ref. 11) or polycrystalline c -BN samples grown by the current vapor phase method, suggesting that these materials are significantly different from the single-crystal counterpart in terms of the sp^3 crystalline content.

In conclusion, we have performed a surface study of a well-characterized single-crystal c -BN. The hydrogenated c -BN (111) shows a 1×1 structure. High-resolution Auger and EELS studies show that the surface of c -BN retains its integrity after hydrogen-plasma treatment, and does not transform to h -BN. The scanning electron microscopy (SEM) study of the hydrogen-plasma-treated surface revealed that the c -BN surface can be effectively etched by hydrogen plasma.

*Author to whom correspondence should be addressed. Electronic address: ando@nirim.go.jp

¹R. F. Davis, Proc. IEEE **79**, 702 (1991).

²J. H. Edgar, J. Mater. Res. **7**, 235 (1992).

³Takashi Sugino, Kazuhiko Tanioka, Seiji Kawasaki, and Junji Shirafuji, Jpn. J. Appl. Phys., Part 2 **36**, L463 (1997).

⁴J. E. Butler and R. L. Woodin, Philos. Trans. R. Soc. London, Ser. A **342**, 209 (1993).

⁵S. J. Harris, A. M. Weiner, G. L. Doll, and W. J. Meng, J. Mater. Res. **12**, 412 (1997).

⁶M. Kagamida, H. Kanda, M. Akaishi, A. Nukui, T. Osawa, and S. Yamaoka, J. Cryst. Growth **94**, 261 (1989).

⁷O. Mishima, S. Yamaoka, and O. Fukunaga, J. Appl. Phys. **61**, 2822 (1987).

⁸B. B. Pate, Surf. Sci. **165**, 83 (1986).

⁹D. R. Penn, J. Electron Spectrosc. Relat. Phenom. **9**, 29 (1976).

¹⁰P. G. Lurie and J. M. Wilson, Surf. Sci. **65**, 453 (1977).

¹¹R. Trhan, Y. Lifschitz, and J. W. Rabalais, J. Vac. Sci. Technol. A **8**, 4026 (1990).

¹²Y. N. Xu and W. Y. Ching, Phys. Rev. B **44**, 7787 (1991).

¹³I. L. Krainsky, G. T. Mearini, V. M. Asnin, H. Sun, M. Foygel, and A. G. Petukhov, Appl. Phys. Lett. **68**, 2017 (1996).

¹⁴H. R. Phillip and E. A. Taft, Phys. Rev. **127**, 159 (1962).